HHS Public Access

Author manuscript

Biochem Biophys Res Commun. Author manuscript; available in PMC 2017 September 23.

Published in final edited form as:

Biochem Biophys Res Commun. 2016 September 23; 478(3): 1074–1079. doi:10.1016/j.bbrc.2016.08.066.

Endothelial sirtuin 1 inactivation enhances capillary rarefaction and fibrosis following kidney injury through Notch activation

Yujiro Kida[a,*], **Joseph A. Zullo**[a,c], and **Michael S. Goligorsky**[a,b,c]

[a]Renal Research Institute, Department of Medicine, New York Medical College, Valhalla, NY, USA

[b]Renal Research Institute, Department of Pharmacology, New York Medical College, Valhalla, NY, USA

[c]Renal Research Institute, Department of Physiology, New York Medical College, Valhalla, NY, USA

Abstract

Peritubular capillary (PTC) rarefaction along with tissue fibrosis is a hallmark of chronic kidney disease (CKD). However, molecular mechanisms of PTC loss have been poorly understood. Previous studies have demonstrated that functional loss of endothelial sirtuin 1 (SIRT1) impairs angiogenesis during development and tissue damage. Here, we found that endothelial SIRT1 dysfunction causes activation of endothelial Notch1 signaling, which leads to PTC rarefaction and fibrosis following kidney injury. In mice lacking functional SIRT1 in the endothelium (Sirt1 mutant), kidney injury enhanced apoptosis and senescence of PTC endothelial cells with impaired endothelial proliferation and expanded myofibroblast population and collagen deposition. Compared to wild-type kidneys, Sirt1 mutant kidneys up-regulated expression of Delta-like 4 (DLL4, a potent Notch1 ligand), Hey1 and Hes1 (Notch target genes), and Notch intracellular domain-1 (NICD1, active form of Notch1) in microvascular endothelial cells (MVECs) post-injury. Sirt1 mutant primary kidney MVECs reduced motility and vascular assembly and enhanced senescence compared to wild-type kidney MVECs. This difference in the phenotype was negated with Notch inhibition. Concurrent stimulation of DLL4 and transforming growth factor (TGF)-β1 increased *trans*-differentiation of primary kidney pericytes into myofibroblast more than TGF-β1 treatment alone. Collectively, these results indicate that endothelial SIRT1 counteracts PTC rarefaction by repression of Notch1 signaling and antagonizes fibrosis via suppression of endothelial DLL4 expression.

Keywords

Endothelial cell; Sirtuin 1; Notch1; Kidney

[*]Corresponding author. Renal Research Institute, Department of Medicine, New York Medical College, 15 Dana Road, Basic Sciences Building, Room C06, Valhalla, NY 10595, USA., yujirokida@gmail.com (Y. Kida).

Disclosures

None.

Transparency document

Transparency document related to this article can be found online at http://dx.doi.org/10.1016/j.bbrc.2016.08.066.

1. Introduction

The kidney has considerable capacity to repair and regenerate. Central to nephron repair and regeneration is repair of peritubular capillaries (PTCs), but kidney PTCs are particularly susceptible to permanent loss after injury [1]. Rarefaction of PTCs, together with interstitial fibrosis, is one of the major hallmarks of chronic kidney disease (CKD) [2]. Animal models of CKD have shown a negative correlation between PTC density and the severity of kidney fibrosis [2]. Moreover, in patients with CKD, the extent of PTC loss predicts the severity of interstitial fibrosis and the decline in renal function [3,4]. Thus, PTC could be a novel therapeutic target to mitigate CKD progression to end stage kidney disease. However, the molecular mechanisms of PTC rarefaction after kidney injury remain poorly understood.

Sirtuin 1 (SIRT1) is an NAD+-dependent deacetylase that is highly expressed in endothelial cells [5]. SIRT1 maintains angiogenic potential of endothelial cells by regulating signaling pathways via its deacetylase activity [6]. Roles of SIRT1 in endothelial cells *in vivo* have been studied using mutant mice, in which SIRT1 lacks its deacetylase activity in the endothelium by deletion of exon 4 (encoding SIRT1 catalytic domain) [7]. These mutant mice (hereafter called Sirt1 mutant mice) demonstrated capillary rarefaction in the microvasculature of neonatal retina and in the hind-limb ischemia model due to impaired angiogenesis [5,8]. In the kidney of Sirt1 mutant mice, impairment of renal function and fibrosis were enhanced following folic acid-induced injury [9], indicating that endothelial SIRT1 protects against kidney injury. However, the mechanisms that afford renal protection are not completely elucidated. SIRT1 represses Notch1 signaling in retinal endothelial cells, which contributes to retinal angiogenesis [8]. We therefore investigated how endothelial SIRT1 counteracts PTC loss and fibrosis during kidney injury through Notch1 signaling.

2. Materials and methods

2.1. In Vivo studies

To delete catalytic domain of SIRT1 protein in endothelial cells, we crossed *Tie2-Cre* mice (the Jackson Laboratory, stock No: 008863, strain: B6) with $Sirt1^{F/F}$ mice (exon 4 of Sirt1 gene is flanked by two loxP sites) (the Jackson Laboratory, stock No: 008041, strain: B6; 129S). Genotyping was performed according to instructions by the company [9]. Resultant Sirt1 mutant mice were subjected to UUO surgery. The surgical procedures were performed as previously described [10]. Mice were euthanized 10 days post-UUO. Contralateral kidneys without injury were served as controls. αSMA-GFP mice (gifted from Ivo Kalajzic) [11] were used for kidney pericyte isolation. Animal protocols were conducted in accordance with the National Institutes of Health guidelines and were approved by the Institutional Animal Care and Use Committee at New York Medical College.

2.2. Tissue preparation and histology

Mouse tissues were prepared and stained as previously described [10]. Briefly, PLP-fixed kidneys were cryo-sectioned and stained with antibodies against primary antibodies. These antibodies include CD31 (1:200; BD Biosciences, #550274), αSMA (1:200; abcam, #ab5694), NICD1 (1:100; abcam, #ab8925), H3K9me3 (1:400; abcam, #ab8898), Ki67

(1:200; abcam, #ab15580), F4/80 (1:200; eBioscience, #14-4801-81) and PDGFRβ (1:400; a gift from William Stallcup). Primary antibodies were detected with either Alexa488- or Alexa-594 conjugated secondary antibodies (1:400; Molecular Probes). PTC density was quantified using CD31-stained sections and grid methods. Fibrosis was assessed using Picrosirius red stained sections and a polarized light. TUNEL reaction was performed by In Situ Cell Death Detection Kit (Roche).

2.3. Quantitative PCR (qPCR)

Total RNA was extracted using TRIzol (Invitrogen). Purity of RNA was determined by A260 to A280 ratio. After cDNA was synthesized, qPCR reaction was performed by Mx3000P qPCR system (Stratagene) and PerfeCta SYBR Green FastMix (Quanta bioscience). Primer sequences were listed in Supplemental Table 1.

2.4. Isolation and culture of cells from kidney

Primary MVECs and pericytes were isolated from adult mouse kidneys using magetic beads based methods. To prepare kidney single cell suspension, kidney was decapsulated, minced, and digested with Collagenase H (1 mg/mL; Roche) and Collagenase/Dispase (1 mg/mL; Roche) in DMEM/F12 medium (Gibco). Single cell suspension was filtered through a cell strainer (40 μm; Fisher Scientific) to remove glomeruli and arterioles, centrifuged, and re-suspended in Isolation Buffer (1 × PBS, 1% BSA). Purified anti-CD31 antibodies (BD Biosciences, #553369) were incubated with Dyna-beads anti-rat IgG (Invitrogen) (4 °C, overnight) prior to cell isolation procedure. Cells were incubated with CD31 antibody-beads complex (4 °C, 1 h). Positive selection was performed by Magnetic Particle Concentrator (Invitrogen). Selected cells were directly applied to RNA isolation or cultured in endothelial medium (IMDM [Gibco], 15% FBS, 1% BSA, 0.01 mg/mL recombinant human insulin, 0.2 mg/mL human transferrin, 100 ng/mL recombinant mouse VEGF, 100 ng/mL recombinant mouse basic FGF, 100 ng/mL recombinant mouse EGF, 1 × penicillin/streptomycin) in 6 cm dish pre-coated with 1% gelatin. High concentration of VEGF (>40 ng/mL) supports selective MVEC growth with high purity [12]. Purity of primary cultures was confirmed by staining for CD31 or VE-cadherin. If its purity was less than 85%, second positive selection was performed. Cells were used between passages 1 and 3.

Primary pericytes were isolated from kidneys of αSMA-GFP mice using abovementioned methods. Kidney single cell suspension was incubated with PDGFRβ antibody-beads complex in Isolation Buffer (4 °C, 1 h). PDGFRβ antibodies (gifted from William Stallcup) were pre-incubated with Dynabeads M-280 anti-rabbit IgG (Invitrogen). Isolated cells were directly applied to RNA isolation or cultured in DMEM/F12 with 10% FBS and 1 × penicillin/streptomycin in 6 cm dish pre-coated with 1% gelatin. High purity of primary cultures (>93%) was confirmed by staining for PDGFRβ. Cells were used between passages 1 and 2.

2.5. Staining of isolated cells

Cells were fixed with cold methanol (4 °C, 15 min) and blocked with 5% BSA/PBS (room temperature, 30 min). Primary antibodies (CD31 [1:200; BD Biosciences], VE-cadherin [1:200; BD Biosciences, #550548], F4/80 [1:200; eBioscience]) were incubated with cells

(4 °C, overnight). Primary antibodies were detected with either Alexa488- or Alexa-594 conjugated secondary antibodies (1:400; Molecular Probes). For senescence-associated β-galactosidase (SA-β-Gal) staining, kidney MVECs were seeded to 24-well plates pre-coated with 1% gelatin and human DLL4 (1 μg/mL; PeproTech) and cultured until 50% confluent. After serum deprivation, MVECs were cultured in IMDM with 0.5% FBS including mouse VEGF (100 ng/mL) for 48 h with DAPT (*N*-[*N*-(3,5-Difluorophenacetyl)-L-alanyl]-*S*-phenylglycine *t*-butyl ester) (γ-secretase inhibitor to suppress NICD generation) (2 μM; abcam, #120633) or its vehicle, DMSO. Cells were fixed with 3% paraformaldehyde (PFA) in PBS (room temperature, 5 min) and stained for SA-β-Gal. Images (×100) were captured and the number of SA-β-Gal+ cells was normalized with total number of nuclei. To assess NICD1 expression, WT or mutant MVECs were seeded to gelatin/DLL4 coated wells. MVECs (50% confluent) were treated with DAPT or DMSO for 48 h after serum deprivation. Cells were fixed with 4% PFA, permeabilized with 0.5% Triton/PBS, and incubated with NICD1 antibodies (1:100). NICD1+ cells were identified by nuclear NICD1 staining.

2.6. Migration assays

Migration of MVECs was assessed using a wound healing assay as described [10] with some modifications. In gelatin/human DLL4-coated 24-well plates, MVECs were cultured until 100% confluent. After serum deprivation, the monolayer of cells was wounded using a 200-μL micropipette tip. After wells were washed with PBS, cells were cultured in IMDM including 0.5% FBS and 100 ng/mL VEGF with DAPT or its vehicle, DMSO for 48 h. Cell free areas were measured using ImageJ software. A percentage of wound closure was calculated by the following formula: [(wound area at time 0 – wound area at 48 h)/wound area at time 0] × 100.

2.7. 2-Dimensional angiogenesis assay

In 24-well plate, WT or Sirt1 mutant kidney MVECs (5×10^4 cells/well) were seeded onto Matrigel (200 μl/well; Corning, #356231) and cultured in IMDM including 2% FBS, 100 ng/mL VEGF, and 1 μg/mL human DLL4 with DAPT (3 μM) or DMSO. After 2 h, the number of endothelial branch point was quantified under ×100.

2.8. Pericyte-to-myofibroblast transdifferentiation assay

PDGFRβ+ pericytes were isolated from kidneys of αSMA-GFP mice [11]. Isolated pericytes (5×10^4 cells/well) were cultured in gelatin-coated 24-well plates with or without human TGF-β1 (5 ng/mL; R&D systems) for 48 h. A part of cells were treated with recombinant human DLL4 (1 μg/mL) for the same period of time. GFP expression was assessed by ImageJ. Total RNA was also isolated from each group of pericytes.

2.9. Statistical analyses

Results are presented as mean ± SEM. We used one-way ANOVA followed by Tukey's HSD *post hoc* test. A P value less than 0.05 was considered significant.

The Supplementary Material provides details of Materials and Methods.

3. Results

3.1. Endothelial inactivation of SIRT1 aggravates capillary loss and tissue fibrosis after kidney injury

First, we subjected Sirt1 mutant mice and wild type (WT) littermates (expressing functional SIRT1 in the endothelium) to a progressive CKD model, unilateral ureteral obstruction (UUO), to assess whether SIRT1 inactivation in microvascular endothelial cells (MVECs) aggravates PTC rarefaction and tissue fibrosis after injury. PTC density was significantly low in Sirt1 mutant kidneys compared to WT kidneys pre- and post-UUO injury (Fig. 1A, B). Following injury, Sirt1 mutant kidneys reduced renal blood flow as well as MVEC proliferation and enhanced MVEC apoptosis compared to WT kidneys (Supplemental Fig. 1A–C). As a functional depletion of SIRT1 is a major cause of endothelial premature senescence [6,13], we also assessed senescence of MVECs by double-staining for CD31 and histone H3 trimethylated lysine 9 (senescence cell marker indicative of repressive heterochromatin structure) [14]. Senescent endothelial cells cease to proliferate [6,15,16]. Both in control and damaged kidneys, the number of senescent MVECs increased in Sirt1 mutant mice compared to WT mice (Supplemental Fig. 1D, E). These findings suggest that apoptosis and senescence of MVECs contribute to enhanced PTC loss in damaged Sirt1 mutant kidneys. Without injury, Sirt1 mutant kidneys expressed abnormally high level of *Vegfa* (encoding vascular endothelial growth factor-A) compared to WT kidneys (Supplemental Fig. 1F), suggesting that Sirt1 mutant MVECs demand large amount of VEGF-A to maintain endothelial architecture. Along with enhanced PTC rarefaction, Sirt1 mutant kidneys increased α-smooth muscle actin (αSMA)+ areas (occupied by scar-forming myofibroblasts) and collagen deposition compared to WT kidneys, which was remarkable after injury (Fig. 1A, C, D, Supplemental Fig. 2A, B). As tissue inflammation is another hallmark of CKD, we assessed infiltration of F4/80+ macrophages into kidneys and detected no difference between WT and mutants (Supplemental Fig. 2C, D). In our UUO model, we found no morphological abnormalities of glomeruli both in WT and Sirt1 mutant kidneys (data not shown). We confirmed that functional loss of endothelial SIRT1 aggravates PTC rarefaction and tissue fibrosis after UUO kidney injury.

3.2. Loss of functional SIRT1 enhances Notch1 signaling in capillary endothelial cells following injury

In retinal MVECs of mouse neonates, activated Notch1 signaling attenuates microvascular angiogenesis [17,18]. Moreover, one recent study demonstrated that SIRT1 deacetylates and destabilizes Notch intracellular domain-1 (NICD1, a cleaved and active form of Notch1), which suppresses Notch1 signaling in retinal MVECs of developing mouse *in vivo* [8]. Therefore, we hypothesized that SIRT1 inactivation augments Notch1 signaling in PTC MVECs. We isolated MVECs from control and UUO kidneys of WT and Sirt1 mutant mice using our methods that exclude arterioles and glomeruli [9,10]. Isolated kidney MVECs were directly subjected to quantitative PCR (qPCR) assays to assess Notch1 signaling. We confirmed genetic deletion of *Sirt1 exon 4* in kidney MVECs of Sirt1 mutant. Expression of *Sirt1 exon 4* was similar between WT and Sirt1 mutant perivascular pericytes (Fig 2A, Supplemental Fig. 2E). Together, this indicates Cre-based target DNA excision in MVEC population. Notably, kidney injury strongly diminished transcripts encoding catalytic

domain of SIRT1 in MVECs of WT kidneys. Delta like 4 (DLL4) is a membrane-bound and predominant ligand for Notch1 receptor [17,19,20]. The mRNA expression of *Dll4* and *Notch1* was elevated in Sirt1 mutant kidneys following injury (Fig. 2B, C) whereas similar levels of *Jagged1*, another less potent ligand for Notch1, were detected between WT and mutant kidneys post-UUO (data not shown). The Notch target genes *Hey1* and *Hes1* were also up-regulated in MVECs of damaged Sirt1 mutant kidneys (Fig. 2D, E). SIRT1 deacetylates and inactivates p53, antagonizing cell senescence [6]. Transcripts of p53 were synergistically increased by endothelial SIRT1 inactivation and kidney injury, supporting the idea that SIRT1 dysfunction and injury induce endothelial senescence (Fig. 2F). Although *Hey1* is reported to repress VEGFR2 expression in human vein endothelial cells [21], we did not detect difference in *Vegfr2* level between WT and Sirt1 mutant MVECs pre- and post-injury (data not shown). Nuclear translocation of NICD1 positively and directly reflects Notch1 signal activity. To assess Notch1 activity *in vivo*, we stained kidney sections using *anti*-NICD1 antibodies, which specifically detect NICD1 but not uncleaved Notch1. Consistent with qPCR results of *Hey1/Hes1*, the number of NICD1+ MVECs was increased in Sirt1 mutant kidneys compared to WT kidneys after injury while no NICD1 expression was detected in non-damaged WT kidneys (Fig. 2G, H).

3.3. Functional loss of SIRT1 impairs angiogenic potential of kidney MVECs via Notch activation in vitro

To evaluate whether activated Notch signaling impairs angiogenic potential of MVECs in Sirt1 mutant kidneys, we isolated and cultured $CD31^+$ MVECs from WT and mutant kidneys. More than 93% of isolated cells were positive for CD31 or VE-cadherin without contamination of F4/80+ macrophages (Fig. 3A). As endothelial migration is involved in angiogeneis, we assessed MVEC migration in response to DLL4 stimulation for Notch1 activation. Genetic or chemical inactivation of SIRT1 repressed migration of MVECs, which was completely restored with Notch inhibitor (DAPT) (Fig. 3B, Supplemental Fig. 3A). Moreover, senescence of kidney MVECs was enhanced by genetic or chemical SIRT1 inactivation, which was fully antagonized with Notch inhibition (Fig. 3C, Supplemental Fig. 3B). Sirt1 mutant MVECs impaired vascular assembly on Matrigel, which was counteracted with DAPT (Fig. 3D, E). Lastly, we confirmed that enhanced NICD1 expression was effectively decreased with DAPT in mutant MVECs (Supplemental Fig. 3C). These results suggest that loss of functional SIRT1 impairs angiogenic potential of kidney MVECs via Notch1 activation.

3.4. Endothelial DLL4 expression triggers pericyte-myofibroblast transition and enhances fibrosis

In vascular smooth muscle cells, Notch1 activation increases αSMA promoter activity and its expression [22]. In bones of developing mice, capillary endothelial DLL4 is essential for expansion of platelet-derived growth factor receptor-β (PDGFRβ)+ perivascular pericytes [23]. Kidney PDGFRβ+ pericytes surround capillary MVECs to stabilize normal vasculature and are identified as a major precursor of αSMA+ myofibroblasts [24]. We confirmed PDGFRβ+ pericyte population expanded more in Sirt1 mutant kidneys than WT kidneys post-UUO (Supplemental Fig. 4A, B). Thus, we hypothesized that endothelial *trans*-membrane ligand, DLL4 locally triggers pericyte-myofibroblast transition as Sirt1 mutant

MVECs showed elevated *Dll4* transcripts following injury (Fig. 2B). We isolated PDGFRβ+ pericytes from kidneys of αSMA-green fluorescent protein (GFP) mice (Supplemental Fig. 4C), in which GFP expression is driven by αSMA promoter [11]. Recombinant DLL4 protein and transforming growth factor (TGF)-β1 synergistically increased expression of αSMA-GFP and type I collagen transcripts (Fig. 4A–C). This suggests that Sirt1 mutant MVECs induce excessive myofibroblast differentiation through increased endothelial DLL4 expression after kidney injury, resulting in enhanced fibrosis.

4. Discussion

Previous study demonstrated that global Sirt1 heterozygous mice (SIRT1 reduction) or mice with tubular NICD1 over-expression (Notch1 augmentation) enhance kidney fibrosis post-UUO [25,26]. Additionally, SIRT1 was shown to directly promote NICD1 degradation in endothelial cells [8]. However, no study has investigated the role of endothelial SIRT1-Notch1 axis in tissue damage. Our results present evidence, for the first time, that dysfunction of endothelial SIRT1 enhances Notch1 signaling, which aggravates kidney injury.

Our study focused on Notch1 signaling as a downstream target of SIRT1 in kidney MVECs. NICD1 over-expression strongly impairs proliferation of human dermal MVECs [27]. In human cardiac MVECs, NICD1 up-regulates DLL4 expression, which further activates Notch1 signaling [20]. SIRT1 directly represses Notch1 promoter activity [28]. These reports support our findings in kidney MVEC. Moreover, SIRT1 antagonizes other anti-angiogenic factors such as FOXO1 and p53 in MVECs of other organs [5,6]. We demonstrated that p53 level increased in Sirt1 mutant MVECs post-UUO, possibly impairing angiogenic potential of MVECs. In the heart, endothelial p53 has a potential to aggravate capillary loss and fibrosis [29].

On the other hand, deletion of Notch1 in collagen-producing cells suppresses myofibroblast differentiation and fibrosis in the lung [30]. This implicates, together with our findings, that DLL4-Notch1 cascade regulates myofibroblast differentiation and fibrosis during tissue injury.

We found that Sirt1 mutant kidneys exhibit abnormally high expression of VEGF-A pre-injury. As VEGF-A from tubular epithelial cells maintains PTC network [31], we speculate that Sirt1 mutant MVECs require large amount of VEGF-A for their survival. Sirt1 MVECs may enhance apoptosis post-UUO injury due to excessive loss of tubular epithelial compartment. Further study is required to determine major regulators of PTC loss and fibrosis in Sirt1 mutant kidneys.

Although endothelial selective SIRT1 activators are currently unavailable, pharmacological SIRT1 activation ameliorates UUO-induced fibrosis [25]. There are ongoing clinical trials on the efficacy of SIRT1 activators on vascular injury [6]. SIRT1 activation could be a promising target to treat CKD patients.

In conclusion, our results indicate that endothelial SIRT1 counteracts PTC rarefaction by repression of Notch1 signaling and antagonizes fibrosis via suppression of endothelial DLL4 expression.

Supplementary Material

Refer to Web version on PubMed Central for supplementary material.

Acknowledgments

The authors thank Michael Potente and Barbara Zimmermann (Max Planck Institute for Heart and Lung Research, Bad Nauheim, Germany) for sharing reagents and advice, William Stallcup (Bur-ham Institute, La Jolla, CA) for *anti*-PDGFRβ antibody, Marta Chris-tov and Brian Ratliff (New York Medial College, Valhalla, NY) for sharing reagents.

This work was supported by the grants from the National Institutes of Health (DK54602, DK052783, and DK45462) and West-chester Artificial Kidney Foundation.

References

1. Basile DP. Rarefaction of peritubular capillaries following ischemic acute renal failure: a potential factor predisposing to progressive nephropathy. Curr Opin Nephrol Hypertens. 2004; 13:1–7. [PubMed: 15090853]
2. Kida Y, Tchao BN, Yamaguchi I. Peritubular capillary rarefaction: a new therapeutic target in chronic kidney disease. Pediatr Nephrol. 2014; 29:333–342. [PubMed: 23475077]
3. Seron D, Alexopoulos E, Raftery MJ, et al. Number of interstitial capillary cross-sections assessed by monoclonal antibodies: relation to interstitial damage. Nephrol Dial Transpl. 1990; 5:889–893.
4. Choi YJ, Chakraborty S, Nguyen V, et al. Peritubular capillary loss is associated with chronic tubulointerstitial injury in human kidney: altered expression of vascular endothelial growth factor. Hum Pathol. 2000; 31:1491–1497. [PubMed: 11150374]
5. Potente M, Ghaeni L, Baldessari D, et al. SIRT1 controls endothelial angiogenic functions during vascular growth. Genes Dev. 2007; 21:2644–2658. [PubMed: 17938244]
6. Kida Y, Goligorsky MS. Sirtuins, Cell senescence, and vascular aging. Can J Cardiol. 2016; 32:634–641. [PubMed: 26948035]
7. Cheng HL, Mostoslavsky R, Saito S, et al. Developmental defects and p53 hyperacetylation in Sir2 homolog (SIRT1)-deficient mice. Proc Natl Acad Sci U S A. 2003; 100:10794–10799. [PubMed: 12960381]
8. Guarani V, Deflorian G, Franco CA, et al. Acetylation-dependent regulation of endothelial Notch signalling by the SIRT1 deacetylase. Nature. 2011; 473:234–238. [PubMed: 21499261]
9. Vasko R, Xavier S, Chen J, et al. Endothelial sirtuin 1 deficiency perpetrates nephrosclerosis through downregulation of matrix metalloproteinase-14: relevance to fibrosis of vascular senescence. J Am Soc Nephrol. 2014; 25:276–291. [PubMed: 24136919]
10. Kida Y, Ieronimakis N, Schrimpf C, et al. EphrinB2 reverse signaling protects against capillary rarefaction and fibrosis after kidney injury. J Am Soc Nephrol. 2013; 24:559–572. [PubMed: 23492730]
11. Yokota T, Kawakami Y, Nagai Y, et al. Bone marrow lacks a transplantable progenitor for smooth muscle type alpha-actin-expressing cells. Stem Cells. 2006; 24:13–22. [PubMed: 16099999]
12. Ligresti G, Nagao RJ, Xue J, et al. A novel three-dimensional human peri-tubular microvascular system. J Am Soc Nephrol. 2016; 27:2370–2381. [PubMed: 26657868]
13. Chen J, Xavier S, Moskowitz-Kassai E, et al. Cathepsin cleavage of sirtuin 1 in endothelial progenitor cells mediates stress-induced premature senescence. Am J Pathol. 2012; 180:973–983. [PubMed: 22234173]
14. Bernardes de Jesus B, Blasco MA. Assessing cell and organ senescence bio-markers. Circ Res. 2012; 111:97–109. [PubMed: 22723221]

15. Erusalimsky JD. Vascular endothelial senescence: from mechanisms to pathophysiology. J Appl Physiol. 2009; 106:326–332. [PubMed: 19036896]
16. Chen J, Goligorsky MS. Premature senescence of endothelial cells: methu-saleh's dilemma. Am J Physiol Heart Circ Physiol. 2006; 290:H1729–H1739. [PubMed: 16603702]
17. Hellstrom M, Phng LK, Hofmann JJ, et al. Dll4 signalling through Notch1 regulates formation of tip cells during angiogenesis. Nature. 2007; 445:776–780. [PubMed: 17259973]
18. Suchting S, Freitas C, le Noble F, et al. The Notch ligand Delta-like 4 negatively regulates endothelial tip cell formation and vessel branching. Proc Natl Acad Sci U S A. 2007; 104:3225–3230. [PubMed: 17296941]
19. Noseda M, Chang L, McLean G, et al. Notch activation induces endothelial cell cycle arrest and participates in contact inhibition: role of p21Cip1 repression. Mol Cell Biol. 2004; 24:8813–8822. [PubMed: 15456857]
20. Caolo V, van den Akker NM, Verbruggen S, et al. Feed-forward signaling by membrane-bound ligand receptor circuit: the case of NOTCH DELTA-like 4 ligand in endothelial cells. J Biol Chem. 2010; 285:40681–40689. [PubMed: 20959466]
21. Holderfield MT, Henderson Anderson AM, Kokubo H, et al. HESR1/CHF2 suppresses VEGFR2 transcription independent of binding to E-boxes. Biochem Biophys Res Commun. 2006; 346:637–648. [PubMed: 16782059]
22. Noseda M, Fu Y, Niessen K, et al. Smooth Muscle alpha-actin is a direct target of Notch/CSL. Circ Res. 2006; 98:1468–1470. [PubMed: 16741155]
23. Kusumbe AP, Ramasamy SK, Itkin T, et al. Age-dependent modulation of vascular niches for haematopoietic stem cells. Nature. 2016; 532:380–384. [PubMed: 27074508]
24. Kida Y, Duffield JS. Pivotal role of pericytes in kidney fibrosis. Clin Exp Pharmacol Physiol. 2011; 38:467–473. [PubMed: 21517936]
25. He W, Wang Y, Zhang MZ, et al. Sirt1 activation protects the mouse renal medulla from oxidative injury. J Clin Investig. 2010; 120:1056–1068. [PubMed: 20335659]
26. Bielesz B, Sirin Y, Si H, et al. Epithelial Notch signaling regulates interstitial fibrosis development in the kidneys of mice and humans. J Clin Investig. 2010; 120:4040–4054. [PubMed: 20978353]
27. Liu ZJ, Xiao M, Balint K, et al. Inhibition of endothelial cell proliferation by Notch1 signaling is mediated by repressing MAPK and PI3K/Akt pathways and requires MAML1. FASEB J. 2006; 20:1009–1011. [PubMed: 16571776]
28. Xie M, Liu M, He CS. SIRT1 regulates endothelial Notch signaling in lung cancer. PloS One. 2012; 7:e45331. [PubMed: 23028940]
29. Gogiraju R, Xu X, Bochenek ML, et al. Endothelial p53 deletion improves angiogenesis and prevents cardiac fibrosis and heart failure induced by pressure overload in mice. J Am Heart Assoc. 2015; 4
30. Hu B, Wu Z, Bai D, et al. Mesenchymal deficiency of Notch1 attenuates bleomycin-induced pulmonary fibrosis. Am J Pathol. 2015; 185:3066–3075. [PubMed: 26358219]
31. Dimke H, Sparks MA, Thomson BR, et al. Tubulovascular cross-talk by vascular endothelial growth factor a maintains peritubular microvasculature in kidney. J Am Soc Nephrol. 2015; 26:1027–1038. [PubMed: 25385849]

Appendix A. Supplementary data

Supplementary data related to this article can be found at http://dx.doi.org/10.1016/j.bbrc.2016.08.066.

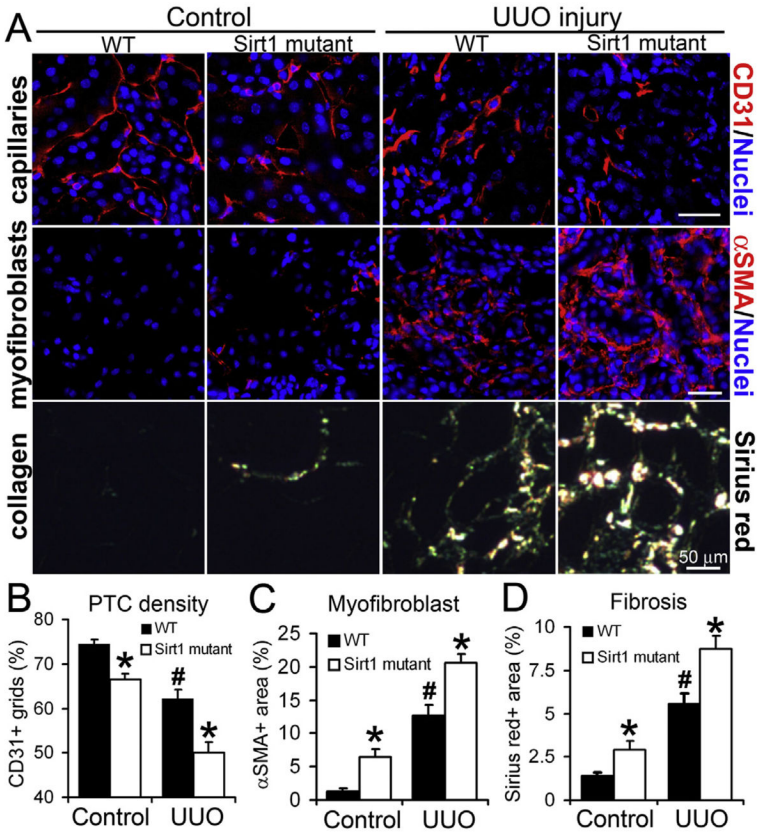

Fig. 1. Endothelial inactivation of SIRT1 aggravates capillary loss and tissue fibrosis after UUO kidney injury

(A) Images of $CD31^+$ capillary endothelial cells, αSMA^+ myofibroblasts, and picrosirius red-stained fibrillar collagens in control and UUO kidneys of WT and Sirt1 mutant mice. **(B)** Quantification of PTC density. $n = 4$ mice/group. **(C)** Quantification of αSMA^+ area. $n = 4$ mice/group. **(D)** Quantification of fibrillar collagen. $n = 4$ mice/group. $*P < 0.05$ vs. corresponding WT group, $\#P < 0.05$ vs. WT control group. Scale bar, 50 μm. (For interpretation of the references to colour in this figure legend, the reader is referred to the web version of this article.)

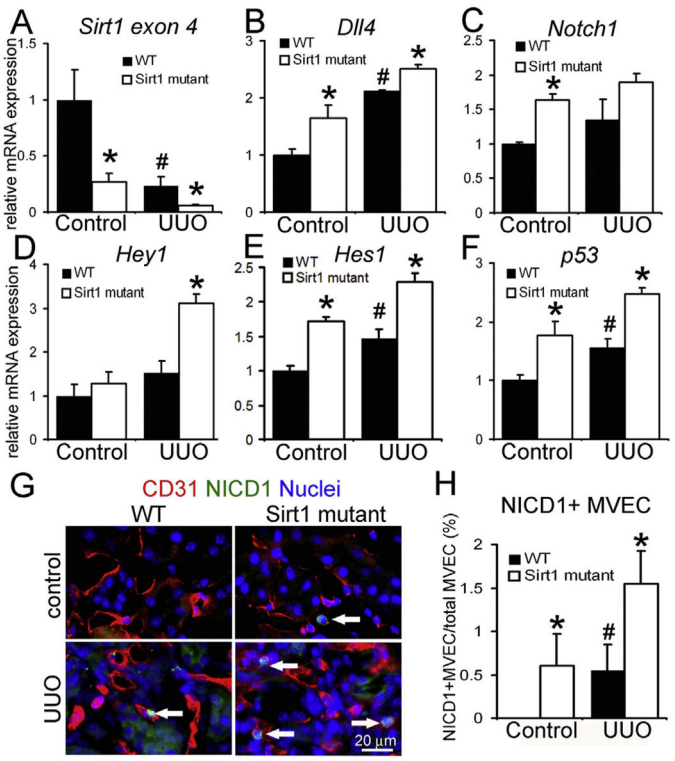

Fig. 2. Loss of functional SIRT1 enhances Notch1 signaling in capillary endothelial cells following UUO kidney injury

qPCR of *Sirt1 exon 4* **(A)**, *Dll4* **(B)**, *Notch1* **(C)**, *Hey1* **(D)**, *Hes1* **(E)** and *p53* **(F)** transcripts in MVECs isolated from control and UUO kidneys of WT and Sirt1 mutant mice. WT: $n = 4$ mice, Sirt1 mutant: $n = 6$ mice. **(G)** Immu-nofluorescence images of $CD31^+$ $NICD1^+$ MVECs in control and UUO kidneys of WT and Sirt1 mutant mice. Arrows indicate double positive cells. **(H)** Quantification of $NICD1^+$ MVECs. Note that no $NICD1^+$ MVECs are detected in control WT kidneys. $n = 4$ mice/group. $*P < 0.05$ vs. corresponding WT group, $\#P < 0.05$ vs. WT control group. Scale bar, 20 μm.

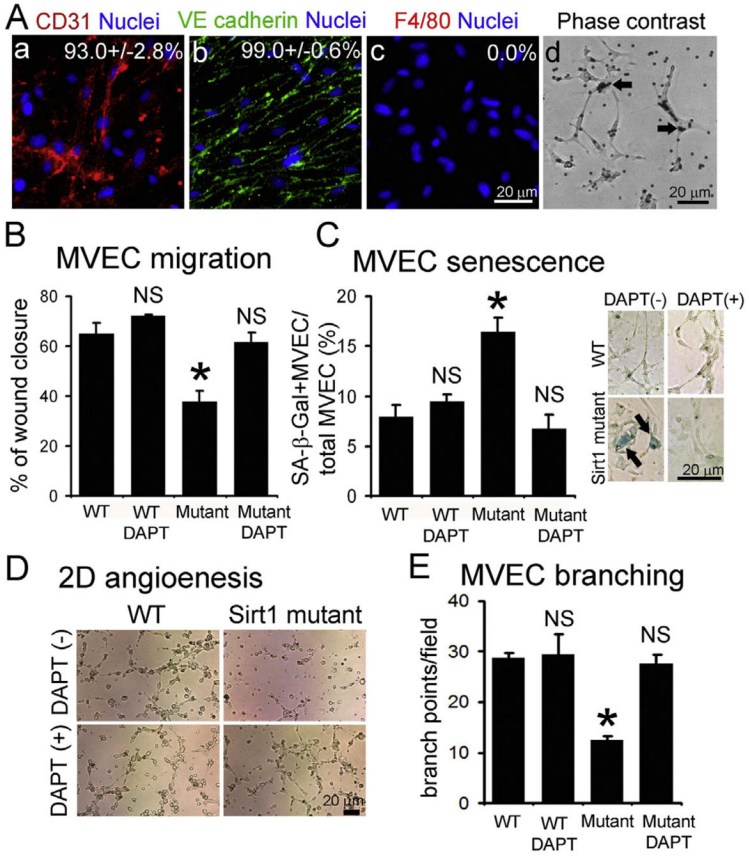

Fig. 3. Functional loss of endothelial SIRT1 impairs angiogenic potential of kidney MVECs via Notch activation

Immunofluorescence images of isolated kidney MVECs stained for CD31 (endothelial marker) **(A–a)**, VE cadherin (endothelial marker) **(A–b)**, and F4/80 (macrophage marker) **(A–c)**. Indicated number means % of positivity for each marker (total 1500 cells from independent two clones). **(A–d)** Phase contrast images of isolated MVECs from WT kidneys. Arrows indicate beads conjugated with CD31 antibodies. **(B)** Migration assay in response to DLL4 and VEGF stimulation using kidney MVECs isolated from WT and Sirt1 mutant (Mutant) mice. Migration is assessed by the percentage of wound closure 48 h after creation of wound in monolayer of cells. Cells are stimulated with DLL4 with Notch inhibitor (DAPT) or its vehicle (DMSO). DAPT is a γ-secretase inhibitor to suppress NICD generation. n = 4/group. **(C)** Kidney MVEC senescence is assessed by senescence-associated β-galactosidase (SA-β-Gal) staining. MVECs isolated from WT and Sirt1 mutant (Mutant) kidneys are stimulated with DLL4 for 48 h with Notch inhibitor (DAPT) or its vehicle (DMSO). n = 4/group. Attached images show results of SA-β-Gal staining using kidney MVECs. Note that SA-β-Gal (blue, arrows) is remarkably detected in Sirt1 mutant MVECs, which is antagonized by concurrent DAPT treatment. **(D)** Images of 2-dimensional (2D) angiogenesis of primary kidney MVECs on Matrigel. Cells are stimulated with DLL4 with Notch inhibitor (DAPT) or its vehicle (DMSO). Images are captured 2 h after seeding of cells onto Matrigel. Note that vascular assembly of Sirt1 mutant MVECs is remarkably impaired, which is counteracted by simultaneous DAPT treatment. **(E)** Quantification of

kidney MVEC branching on Matrigel. $n = 3$/group. $*P < 0.05$ vs. WT control, NS: no significant difference vs. WT control. Scale bar, 20 μm. (For interpretation of the references to colour in this figure legend, the reader is referred to the web version of this article.)

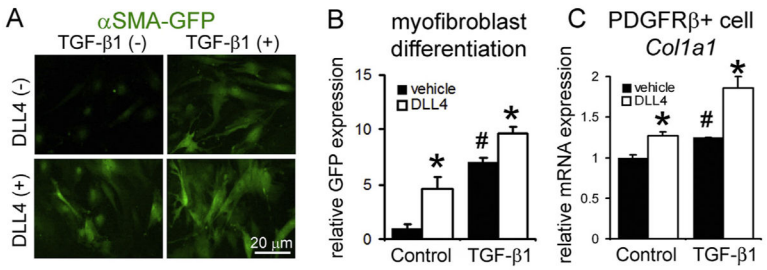

Fig. 4. DLL4 induces pericyte-myofibroblast transition and fibrosis

(A) Images of αSMA-GFP expression in primary kidney PDGFRβ+ pericytes 48 h after indicated treatments. Primary kidney pericytes are isolated from αSMA-GFP mice. Note that DLL4 and TGF-β1 synergistically enhance αSMA-GFP expression. **(B)** Quantification of GFP expression. **(C)** qPCR of collagen I, α1 (*Col1a1*) transcripts in kidney PDGFRβ+ pericytes. $n = 3$/group. $*P < 0.05$ vs. corresponding vehicle treated group, $\#P < 0.05$ vs. vehicle treated control group. Scale bar, 20 μm.